

Analysis of Carrier Heating Effects in Quantum Well Semiconductor Optical Amplifiers Considering Holes' Non-parabolic Density of States

Xia, Mingjun; Ghafouri-Shiraz, Hooshang

DOI:

[10.1007/s11082-014-0049-2](https://doi.org/10.1007/s11082-014-0049-2)

License:

Other (please specify with Rights Statement)

Document Version

Peer reviewed version

Citation for published version (Harvard):

Xia, M & Ghafouri-Shiraz, H 2015, 'Analysis of Carrier Heating Effects in Quantum Well Semiconductor Optical Amplifiers Considering Holes' Non-parabolic Density of States', *Optical and Quantum Electronics*, vol. 47, no. 7, pp. 1847-1858. <https://doi.org/10.1007/s11082-014-0049-2>

[Link to publication on Research at Birmingham portal](#)

Publisher Rights Statement:

The final publication is available at Springer via: <http://dx.doi.org/10.1007/s11082-014-0049-2>.

Checked July 2015

General rights

Unless a licence is specified above, all rights (including copyright and moral rights) in this document are retained by the authors and/or the copyright holders. The express permission of the copyright holder must be obtained for any use of this material other than for purposes permitted by law.

- Users may freely distribute the URL that is used to identify this publication.
- Users may download and/or print one copy of the publication from the University of Birmingham research portal for the purpose of private study or non-commercial research.
- User may use extracts from the document in line with the concept of 'fair dealing' under the Copyright, Designs and Patents Act 1988 (?)
- Users may not further distribute the material nor use it for the purposes of commercial gain.

Where a licence is displayed above, please note the terms and conditions of the licence govern your use of this document.

When citing, please reference the published version.

Take down policy

While the University of Birmingham exercises care and attention in making items available there are rare occasions when an item has been uploaded in error or has been deemed to be commercially or otherwise sensitive.

If you believe that this is the case for this document, please contact UBIRA@lists.bham.ac.uk providing details and we will remove access to the work immediately and investigate.

Analysis of Carrier Heating Effects in Quantum Well Semiconductor Optical Amplifiers Considering Holes' Non-parabolic Density of States

Mingjun Xia and H. Ghafouri-Shiraz

Abstract This paper studies effects of carrier heating on the amplified pico-second Gaussian pulse propagation in a quantum well semiconductor optical amplifier (QW-SOA) taking into account the holes' non-parabolic density of states. In the analysis we have also considered the discontinuous distribution of energy band structure and the coupling between heavy hole (HH), light hole (LH) and spin-orbit split-off (SO) bands. It has been found that at higher temperatures the wavelength at which the peak value of modal gain occurs decreases (small blue shift). The pulse amplification performances of QW-SOAs for two unchirped Gaussian input pulses having the peak power values of $10mw$ and $100mw$ have been investigated both in the presence and absence of the carrier heating effects. It has been found that carrier heating effects broaden the amplified output signal pulse width and lower the peak value of the amplified output pulse.

Keywords Carrier heating effects, holes' density of states, quantum well, semiconductor optical amplifiers, ultra-short pulse amplification

1. Introduction

Due to the potential application in the high-speed optical fiber communication network and all-optical signal processing, there has been a considerable research interest in QW-SOAs (Juodawilkis et al. 2009; Huang et al. 2011; Sun et al. 2013; Qasaimeh 2008; Qin et al. 2012). Semiconductor optical amplifiers have many advantages including small size, wide wavelength range and direct current pumping. However, the high-speed propagation of the pulse signal suffers from distortion due to the gain saturation mechanism. Moreover, carrier heating effects imposes a further constrain on the gain dynamics (Tolstikhin and Willander 1990; Mørk 1994; Mørk 1996). The study of carrier heating effects on pulse amplification is important for understanding of the high-speed application of QW-SOAs.

The nonlinear gain in semiconductor optical amplifiers (SOAs) has been studied for various applications (Huang et al. 2011; Agrawal and Olsson 1989; Ghafouri-Shiraz 1997; Zhou 2008; Xu 2011; Mørk 1996). However, in some reported studies the effects that carrier heating has on the performance of amplifiers have not been considered. Carrier heating effects maintain electrons and holes at a different temperature with the lattice. Temperature changes lead to the different Fermi-Dirac distributions in the conduction and valence bands. This causes gain suppression in the optical pulse amplification. Besides, J.M. Dailey et. (Dailey and Koch 2006; Dailey and Koch 2007) have experimentally illustrated the impact of carrier heating on the dynamic recovery process of SOA. Their experimental results show that the carrier heating not only induces the suppression of material gain but also can accelerate the carrier dynamic recovery. Thus, a systematic theoretical model of SOAs under carrier heating effects is necessary.

In QW-SOAs, the distribution of energy band structure is discontinuous and also due to the coupling among heavy hole bands, and light hole bands as well as spin-orbit split-off bands, the valence band structure is non-parabolic. Thus, the Fermi-Dirac approximation (Dailey and Koch 2007) cannot be adopted to analyse carrier heating effects in QW-SOAs. In this paper, we present a new method

Mingjun Xia

School of Electronic, Electrical and Computer Engineering, University of Birmingham
Birmingham, B15 2TT, UK
e-mail: MXX322@bham.ac.uk

H. Ghafouri-Shiraz (Corresponding author)

School of Electronic, Electrical and Computer Engineering, University of Birmingham
Birmingham, B15 2TT, UK
e-mail: ghafourh@bham.ac.uk

to analyse the carrier heating effects in QW-SOAs where the in-plane wave vector functions have been used to express the energy densities in both conduction and valence bands. Based on the analysis of energy band structure in QW-SOAs we have obtained derivatives of energy density, U , with respect to both temperature (dU/dT) and carrier density (dU/dN). To illustrate the effects of carrier heating on picosecond pulse amplification, we analyse the modal gain spectra and spontaneous emission spectra at different temperatures. Finally, we have investigated the carrier heating effects on picosecond pulse amplification in QW-SOAs for different input pulses. To best of our knowledge, this is the first time that the peculiarity of the quantum well is considered in the calculations of carrier heating effects due to the non-parabolic density of states for the holes.

We organize the paper as follows. Section 2 presents the theory of carrier heating effects, the energy band structure and optical process modelling in QW-SOAs. In Section 3, the energy band structure of a compressively strained quantum well amplifier, the modal gain and spontaneous emission spectra at different temperatures and the effects of carrier heating on the Gaussian picosecond pulse amplification in QW-SOAs are presented. Finally, the conclusion is given in Section 4.

2 Theory

2.1 Carrier heating effects

Assuming the temperature of electrons and holes, T is equal, the carrier temperature dynamics in QW-SOAs can be expressed as (Dailey and Koch 2006; Dailey and Koch 2007; Dailey and Koch 2009; Qin et al. 2011):

$$\frac{dT}{dt} = \frac{1}{\partial U / \partial T} \left(\frac{dU}{dt} - \frac{\partial U}{\partial N} \frac{dN}{dt} \right) - \frac{T - T_0}{\tau} \quad (1)$$

Where, both dN/dt and dU/dt can be obtained from the following carrier density rate equation and the total carrier energy density rate equation (Dailey and Koch 2009; Qin et al. 2011):

$$\begin{aligned} \frac{dN}{dt} = & \frac{I}{qV} - \Gamma \nu_g \sum_{\nu_i} g(N, \nu_i) (S_{\nu_i}^+ + S_{\nu_i}^-) - \\ & \Gamma \nu_g \sum_{\nu_j} g(N, \nu_j) (E_{\nu_j}^+ + E_{\nu_j}^-) - AN - BN^2 - CN^3 \end{aligned} \quad (2)$$

and

$$\begin{aligned} \frac{dU}{dt} = & -\nu_g \sum_i (h\nu_i - E_g(N)) g(N, \nu_i) (S_{\nu_i}^+ + S_{\nu_i}^-) + \\ & \nu_g \alpha_{FC} N \sum_i h\nu_i (S_{\nu_i}^+ + S_{\nu_i}^-) - \\ & \nu_g \sum_j (h\nu_j - E_g(N)) g(N, \nu_j) (E_{\nu_j}^+ + E_{\nu_j}^-) + \\ & \nu_g \alpha_{FC} N \sum_j h\nu_j (E_{\nu_j}^+ + E_{\nu_j}^-) \end{aligned} \quad (3)$$

In the above equations, U is the total carrier energy density, τ is the electron phonon interaction time, T_0 is the lattice temperature, q is the electron charge, V is the volume of the active region, I is the injected current, Γ is the optical confinement factor, ν_g is the group velocity, g is the material gain, ν_i and ν_j are, respectively, the optical input signal and the optical amplifier frequencies.

$S_{\nu_i}^+$ and $S_{\nu_i}^-$ are the forward and backward propagating signals photon densities at the frequencies of interest while $E_{\nu_j}^+$ and $E_{\nu_j}^-$ are the forward and backward photon densities due to the amplified spontaneous emission (ASE) of the amplifier. Parameters, E_g , A , B , C and α_{FC} are, respectively, the band-gap energy, linear, Bi-molecular, Auger recombination and the free carrier absorption cross-section, h is the Plank constant. The propagation of the incident optical signal within the optical amplifier can be expressed as (Dailey and Koch 2009; Qin et al. 2011):

$$\left(\frac{\partial}{\partial t} \pm \nu_g \frac{\partial}{\partial z} \right) S_{\nu_i}^{\pm} = \nu_g S_{\nu_i}^{\pm} (\Gamma g(N, \nu_i) - \alpha_0) \quad (4)$$

Where, α_0 is the waveguide loss. Since the bandwidth of the ASE is larger than that of the optical signal we can express the ASE propagation equation as:

$$\left(\frac{\partial}{\partial t} \pm v_g \frac{\partial}{\partial z}\right) E_{v_j}^{\pm} = v_g E_{v_j}^{\pm} (I g(N, v_j) - \alpha_0) + R_{sp}(v_j, N) \quad (5)$$

Where, R_{sp} is the spontaneous emission rate. The photon densities $S_{v_j}^{\pm}$ and $E_{v_j}^{\pm}$ can be obtained by solving Eq. (4) and (5) using the step-transition method (Ghafouri-Shiraz and Tan 1996). Then these densities can be used in Eq. (2) and (3) to calculate the rate of change of carrier density dN/dt and the rate of change of carrier energy density dU/dt . Since the distribution of energy band structure in a QW-SOA is discontinuous, the analysis of carrier heating effect needs to be considered in 2-D system. Moreover, due to the mixing effects among heavy-hole bands, light-hole bands and spin-orbit split-off bands as well as the strain effects in the valence band, the density of states is not constant for a certain sub-band. Thus, the parabolic band model reported in (O'Reilly et al. 1994) cannot be used to analyse the energy band structure in valence band. These make the computation of the carrier heating effects in QW-SOAs more complex. Hence, in this paper, we have used numerical method to investigate the carrier heating effects. The electron (N) and hole (P) densities in the conduction and valence bands can be expressed as (Chuang 1995):

$$N = \sum_n \frac{1}{\pi L_z} \int_0^{+\infty} f(E_n^c(k_t)) k_t dk_t \quad (6)$$

$$P = \sum_m \sum_{HH, LH, SO} \frac{1}{\pi L_z} \int_0^{+\infty} f(E_m^v(k_t)) k_t dk_t \quad (7)$$

Where, $f(E)$ is the Fermi-Dirac distribution function, $k_t = \sqrt{k_x^2 + k_y^2}$, k_x and k_y are the wave vectors in the x and y directions, L_z is the quantum well width, $E_n^c(k_t)$ is the n th sub-band energy in the conduction band and $E_m^v(k_t)$ is the m th HH, LH and SO sub-band energy in the valence band. The total carrier energy density (U) is the sum of the carrier energy densities of the conduction (U_C) and valence (U_V) bands as (Chuang 1995):

$$U = U_C + U_V \quad (8)$$

Where

$$U_C = \sum_n \frac{1}{\pi L_z} \int_0^{+\infty} \frac{E_n^c(k_t) - E_c}{1 + \exp((E_n^c(k_t) - E_{f_c})/K_B T)} k_t dk_t \quad (9)$$

$$U_V = \sum_m \sum_{HH, LH, SO} \frac{1}{\pi L_z} \int_0^{+\infty} \frac{E_v - E_m^v(k_t)}{1 + \exp((E_{f_v} - E_m^v(k_t))/K_B T)} k_t dk_t \quad (10)$$

K_B is the Boltzmann constant, E_{f_c} and E_{f_v} are the quasi-Fermi levels in the conduction and valence bands, and E_c and E_v are their band edges. Equations (8) to (10) can be used to calculate both $(\partial U / \partial T)$ and $(\partial U / \partial N)$.

2.2 QW-SOAs model

Based on the above analysis, in order to calculate the carrier heating effects in a quantum well SOA we need to calculate both the conduction band $E_n^c(k_t)$ and valence band $E_m^v(k_t)$ sub-band energies, material gain and spontaneous emission rate. Both $E_n^c(k_t)$ and $E_m^v(k_t)$ are determined by solving the following Schrodinger equations, respectively (Chuang 1995):

$$H^c \phi_n(z; k_t) = E_n^c(k_t) \phi_n(z; k_t) \quad (11)$$

$$\sum_{j=HH, LH, SO} H_{3 \times 3, ij}^{\sigma} g_{m, j}^{\sigma}(z; k_t) = E_{\sigma, m}^v(k_t) g_{m, i}^{\sigma}(z; k_t) \quad (12)$$

where, H^c and $H_{3 \times 3,ij}^\sigma$ are the Hamiltonians for the conduction and valence bands, respectively, $\phi_n(z; k_t)$ is the envelope function of the n th conduction sub-band, σ is the upper and lower matrix signs in the block diagonal Hamiltonian for the valence band and $g_{m,j}^\sigma$ is the hole envelope function. In Eq. (12), the strain-dependent coupling between HH, LH and SO bands has been considered in order to obtain the valence-band energy (Chang and Chuang 1995; Sugawara et al. 1993; Chao and Chuang 1992).

In the presence of strain, the Hamiltonian in the conduction band can be expressed as (Chang and Chuang 1995; Sugawara et al. 1993; Chao and Chuang 1992; Chuang 1991):

$$H^c = \left(\frac{\hbar^2}{2} \right) \left(\frac{k_t^2}{m_{e,t}} + \frac{k_z^2}{m_{e,z}} \right) + V_c(z) + a_c \gamma(\bar{\varepsilon}) \quad (13)$$

Where

$$V_c(z) = V_h(z) + E_g \quad (14)$$

$$\gamma(\bar{\varepsilon}) = \varepsilon_{xx} + \varepsilon_{yy} + \varepsilon_{zz} \quad (15)$$

$$\varepsilon_{xx} = \varepsilon_{yy} = \frac{a_0 - a}{a} \quad (16)$$

$$\varepsilon_{zz} = -\frac{2C_{12}}{C_{11}} \varepsilon_{xx} \quad (17)$$

$$\varepsilon_{xy} = \varepsilon_{yz} = \varepsilon_{zx} = 0 \quad (18)$$

In the above equations, \hbar is the Plank constant divided by 2π , k_t and k_z are wave vectors in the perpendicular and parallel to the growth directions, respectively, $V_c(z)$ is the potential energy of the unstrained conduction band edge, $V_h(z)$ is the unstrained valence band edge, E_g is the bandgap in the well, a_c is the hydrostatic deformation potential for the conduction band, $\gamma(\bar{\varepsilon})$ is the fractional volume change, ε_{xx} , ε_{yy} and ε_{zz} are the strain components, $m_{e,t}$ and $m_{e,z}$ are the electron effective masses in the perpendicular and parallel to the growth directions, respectively, a_0 and a are the substrate and the layer material lattice constants, C_{11} and C_{12} are the stiffness constants.

Both the conduction and valence band energies are obtained from Eq. (11) and (12) using the finite difference method (Chang and Chuang 1995). In calculations, we have taken the unstrained valence band edge in the well as the reference energy. The conduction and valence band edges in the barrier are determined by the model-solid theory (Chuang 1991). For the conduction band, Eq. (11) is first solved at $k = 0$ and then by ignoring the non-parabolic effects, we have obtained the whole conduction band energy using the following expression (Zory JR 1993):

$$E_n^c(k_t) = E_n^c(k_t = 0) + \frac{\hbar^2 k_t^2}{2m_{e,t}} \quad (19)$$

For the valence band, the energy band structure can be obtained by substituting $k_z = -i\partial/\partial z$ into the Hamiltonian and applying the finite difference method.

Besides the band structures of quantum well, the material gain $g(\omega)$ and the spontaneous emission rate $R_{sp}(\omega)$ are used to express the optical signal propagation in the amplifier cavity. The material gain of QW-SOAs derived from the Fermi's golden rule can be written as (Chuang 1995):

$$g(\omega) = \frac{q^2 \pi}{n_r c \varepsilon_0 m_0^2 \omega L_z} \sum_{\eta=\uparrow, \downarrow} \sum_{\sigma=U, L} \sum_{n, m} \int |\hat{e} \cdot M_{nm}^{\sigma\eta}|^2 \times \frac{(f_n^c(k_t) - f_{\sigma n}^v(k_t)) (\hbar\gamma)}{4(E_{\sigma, nm}^{cv}(k_t) - \hbar\omega)^2 + (\hbar\gamma)^2} \frac{k_t dk_t}{\pi^2} \quad (20)$$

Where,

$$f_n^c(k_t) = 1 / (1 + \exp(\frac{E_n^c(k_t) - E_{fc}}{K_B T})) \quad (21)$$

$$f_{\sigma n}^v(k_t) = 1 / (1 + \exp(\frac{E_{\sigma, m}^v(k_t) - E_{fv}}{K_B T})) \quad (22)$$

$$E_{\sigma, nm}^{cv}(k_t) = E_n^c(k_t) - E_{\sigma, m}^v(k_t) \quad (23)$$

In the above equations, n_r is the ground refractive index, c is the speed of light in free space, m_0 is the electron rest mass in free space, q is the magnitude of the electron charge, ϵ_0 and γ are the permittivity in free space and the linewidth of the Lorentzian function, respectively, \hat{e} is the polarization vector of the optical electric field, $M_{nm}^{\eta\sigma}$ is the momentum matrix element. The quasi-Fermi levels in the conduction band (E_{fc}) and valence band (E_{fv}) are calculated using the dichotomy method (Kendall 1989). Also, the carrier temperature in Eqs.(21) and (22) is calculated using Eq. (1). The spontaneous emission rate given in Eq.(5) can be obtained by integrating the spontaneous emission spectrum, $r_{sp}(\hbar\omega)$, over the whole optical energy that is (Qin et al. 2011; Jongwoon et al. 2005):

$$R_{sp} = \int r_{sp}(\hbar\omega)d(\hbar\omega) \quad (24)$$

where

$$r_{sp}(\hbar\omega) = \frac{q^2 n_r \omega}{\pi \hbar c^3 \epsilon_0 m_0^2 L_z} \sum_{\eta=\uparrow, \downarrow} \sum_{\sigma=U, L} \sum_{n, m} \int |M_{sp}(k_t)|^2 \times \frac{(f_n^c(k_t) - f_{\sigma m}^v(k_t))(\hbar\gamma)}{4(E_{\sigma, nm}^{cv}(k_t) - \hbar\omega)^2 + (\hbar\gamma)^2} \frac{k_t dk_t}{\pi^2} \quad (25)$$

In Eq. (25), $|M_{sp}(k_t)|$ is the momentum matrix element of the spontaneous emission, which is calculated through the TE polarization component and the TM polarization component. The spontaneous emission rate can be obtained by integrating the spontaneous emission spectrum over the whole optical energy.

3 Results and discussions

In the following first we have investigated the energy band structure, modal gain and spontaneous emission spectra at different temperatures of a QW-SOA and then picosecond pulse amplification. The parameters used in the analysis are given in Table 1.

Table 1
Modelling parameters (Dailey and Koch 2009; Qin et al. 2011)

Symbol	Description	Value
n	Background refractive index	3.6
α_{FC}	Free carrier absorption cross-section	$0.5 \times 10^{-21} m^2$
A	Linear recombination	$2 \times 10^8 s^{-1}$
B	Bi-molecular recombination	$6 \times 10^{-16} m^3 s^{-1}$
C	Auger recombination	$8 \times 10^{-41} m^6 s^{-1}$
τ	Electron phonon interaction time	1ps
α_0	Waveguide loss	$1000 m^{-1}$
Γ	Confinement factor	0.025
N_0	Transparent carrier density	$1.2 \times 10^{24} m^{-3}$
I	Input current	300mA
r	Facet reflectivity	0.001
W	SOA width	1 μm
D	SOA thickness	24.5nm
L	SOA length	750 μm

3.1 Energy band, modal gain and spontaneous emission spectra

The well and barrier materials of the QW-SOA used in the following analysis are $In_{0.64}Ga_{0.36}As$ and $InGaAsP$, respectively, lattice matched to InP substrate. The barrier band-gap wavelength is $\lambda = 1.15\mu m$ and the well and barrier widths are $4.5nm$ and $10nm$. Fig. 1 (a) and (b) show the conduction and valence bands of a compressively strained QW-SOA as a function of the transverse wave vector. In the numerical simulation, the energy of the unstrained valence band edge ($V_h(z)$) is taken as zero.

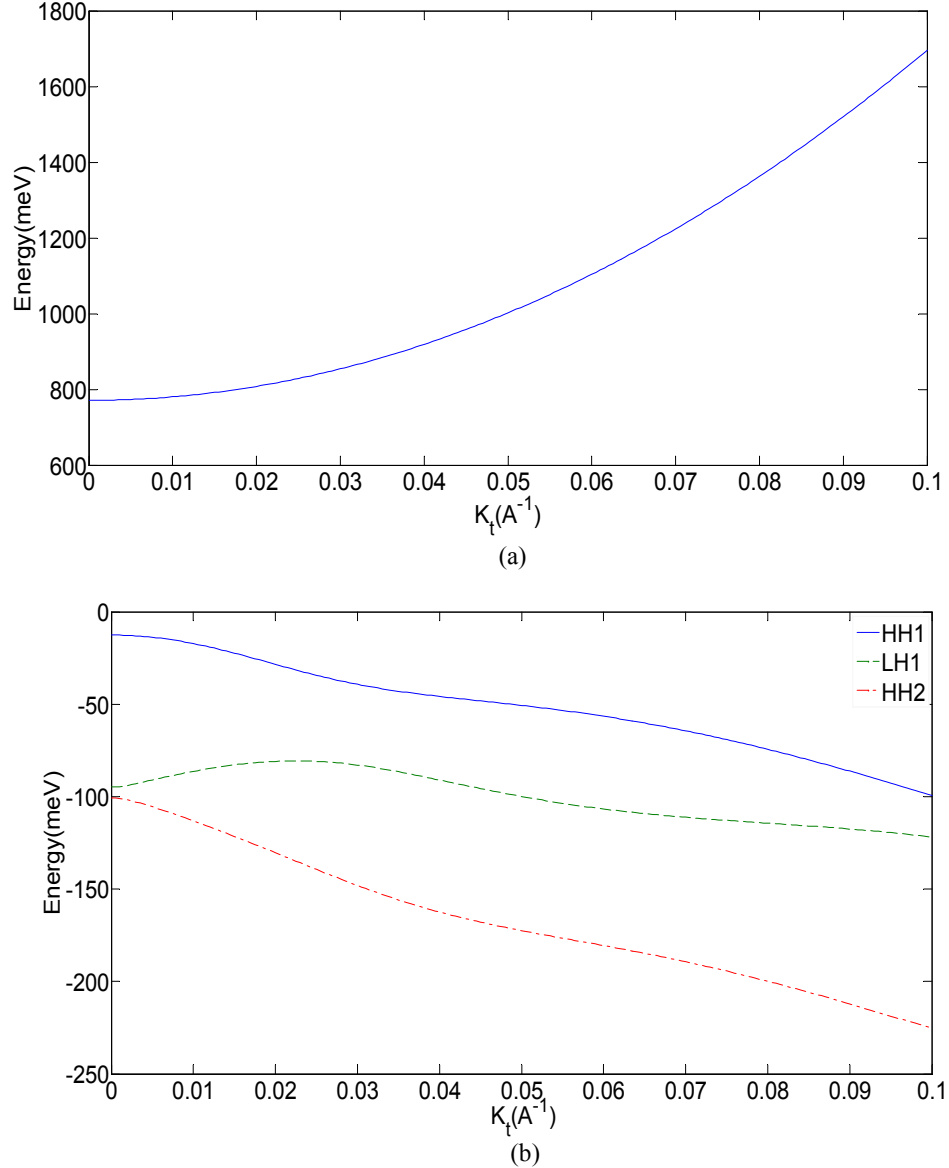


Fig. 1 Energy band structure of a compressively strained QW-SOA (a) conduction band structure (b) valence band structure

Figure 1 shows that the energy in the conduction band varies parabolically with the resultant wave vector k_t . Figure 1(b) clearly shows that the band structure in the valence is non-parabolic due to the strain-dependent coupling among heavy holes bands, light holes bands and spin-orbit bands. Since the energy band structure is discontinuous and the valence band structure is non-parabolic for QW-SOAs, the Fermi-Dirac approximation cannot be applied to calculate the carrier heating effects in QW-SOAs. Therefore, in this paper as explained in Section 2(A) we have applied a new calculation method without using Fermi-Dirac approximation.

Furthermore, the modal gain spectra of the compressively strained QW-SOA for the TE mode polarization at different temperatures are shown in Fig. 2. The carrier density is $8.0 \times 10^{24} m^{-3}$. The peak of the TE modal gain is near $1550nm$, which is low loss for optical fiber communication. Figure 2 shows that the modal gain spectrum is pushed down as the temperature increases. This is because the Fermi-levels in the conduction and valence bands are temperature dependent. When the temperature increases, the

Fermi-level in the conduction band decreases, while the Fermi-level in the valence band increases. The changes of Fermi-levels lead to the reduction of the carrier occupation level. At the same time, the peak of modal gain spectrum shifts to the shorter wavelength when the temperature is higher. The peak wavelengths of the modal gain spectrum are, respectively, $1544.61nm$ ($T = 300K$), $1544.50nm$ ($T = 350K$) and $1544.28nm$ ($T = 400K$). This indicates that as the temperature increases, the modal gain peak wavelength has a small blue shift.

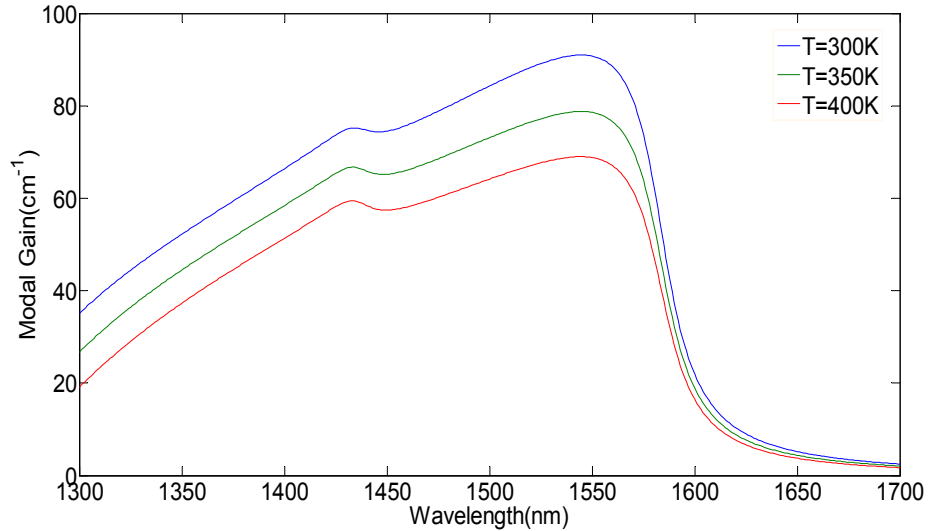


Fig. 2 Modal gain spectra of TE mode for the compressively strained QW-SOA with different temperatures at $N = 8.0 \times 10^{24} m^{-3}$

The spontaneous emission spectra ($qL_z r_{sp}$) is plotted in Fig. 3. In the simulation, again the carrier density is $N = 8.0 \times 10^{24} m^{-3}$. The figure shows that as the temperature increases the spontaneous emission spectra values decreases but the 3-dB bandwidths increases. This is because of changes in quasi-Fermi level due to the different temperatures which results in having different density of states distributions.

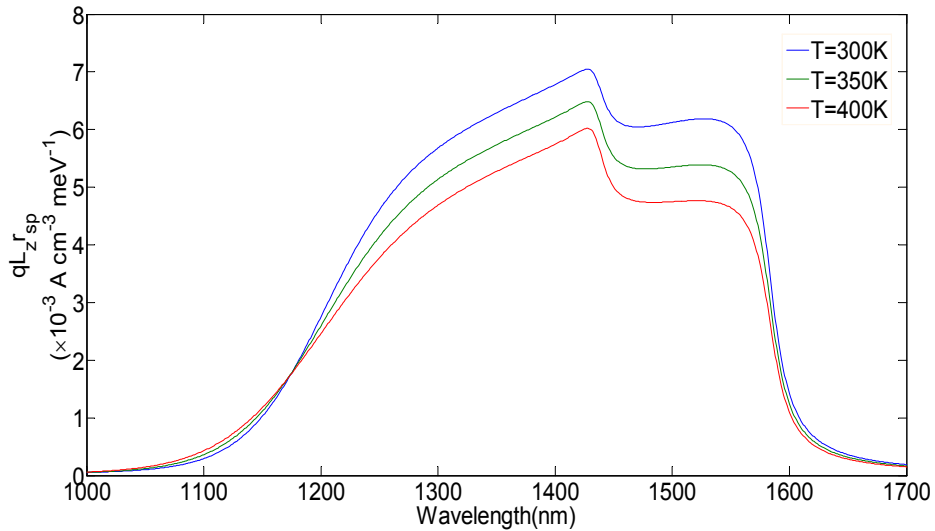


Fig. 3 The spectra of $qL_z r_{sp}$ for the strained QW-SOA with different temperatures at $N = 8.0 \times 10^{24} m^{-3}$

3.2 Picosecond pulse amplification

In the following study, we explore the influences of carrier heating on the QW-SOAs picosecond pulse amplification based on the theoretical analysis explained in section II. The input signals used in our simulations were two ideal Gaussian pulses, namely GP-1 and GP-2, both having the same FWHM of 2ps but different peak values of $10mw$ (GP-1) and $100mw$ (GP-2) both centred at 3ps. The

operating wavelength of the input pulses is 1550nm . In the simulations, the QW-SOA cavity length is divided into 200 sections and for each section, the travelling wave rate equation and the required boundary conditions (Connelly 2001) have been used to analyse the optical field propagation within the cavity. All other parameters used in the simulation are listed in Table-1. Figure 4 shows the pulse amplification responses of input GP-1 both with and without considering the carrier heating effects. The time origin in x-axis means the signal begins to exit the amplifier.

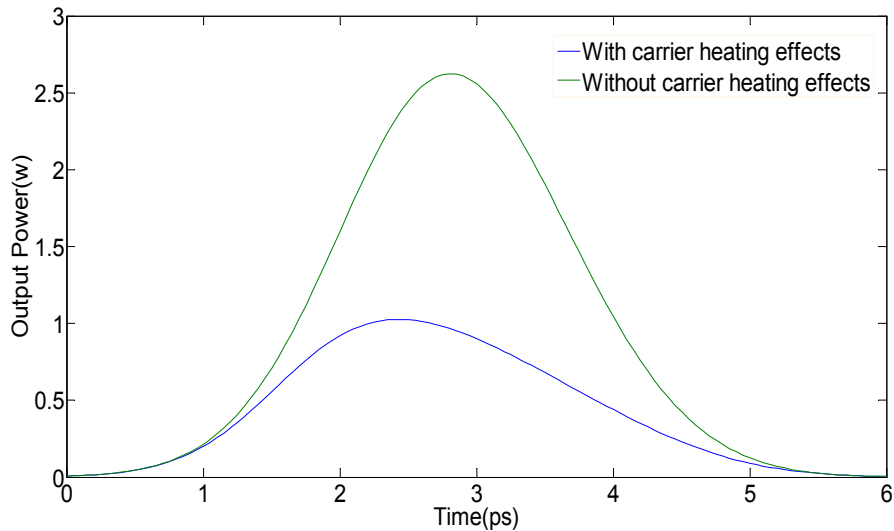


Fig.4 QW-SOAs picosecond pulse amplification (input peak value 10mw) with and without carrier heating effects

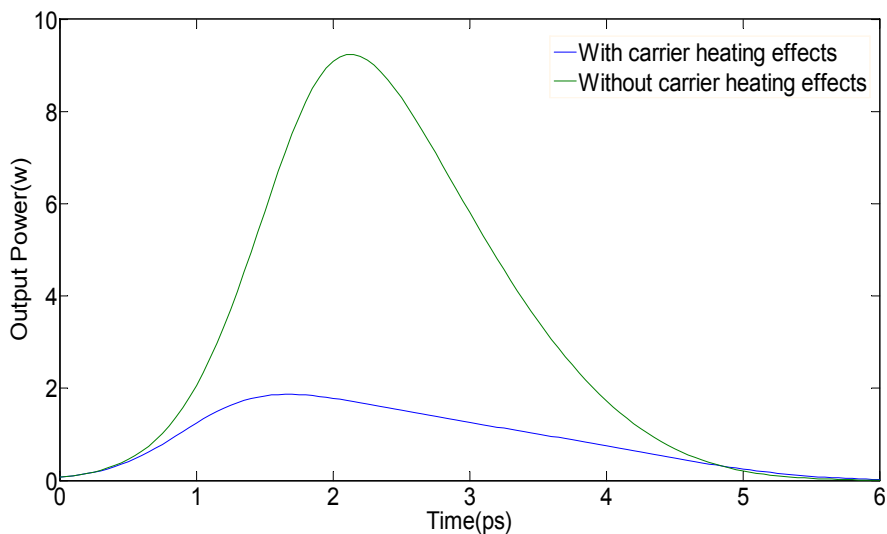


Fig.5 QW-SOAs picosecond pulse amplification (input peak value 100mw) with and without carrier heating effects

The figure shows that the carrier heating effects have reduced the output signal peak power from 2.62W to 1.03W and increased its FWHM from 2ps to 2.40ps . This is because of material gain reduction due to the carrier heating effects as explained in Fig. 2. Moreover, less amplification occurs in the leading edge and around the peak region. On the other hand, when the trail edge of the pulse signal arrives a small number of carriers are depleted so that the gain coefficient remains high. However, when the carrier heating effects are not considered the amplification in the leading edge depletes more carrier density due to the higher gain. The gain coefficient decreases sharply after the leading edge amplification. Therefore, the output signal FWHM is narrower than the input signal.

Figure-5 shows similar results for the input signal GP-2. In this case the output signal peak value has decreased from 9.23W to 1.87W and its FWHM value has increased from 1.9ps to 2.8ps due to carrier heating effects. Comparison of Fig. 4 and 5, indicates that when carrier heating effects are considered the higher the input pulse power, the broader the pulse width of the amplified output pulse

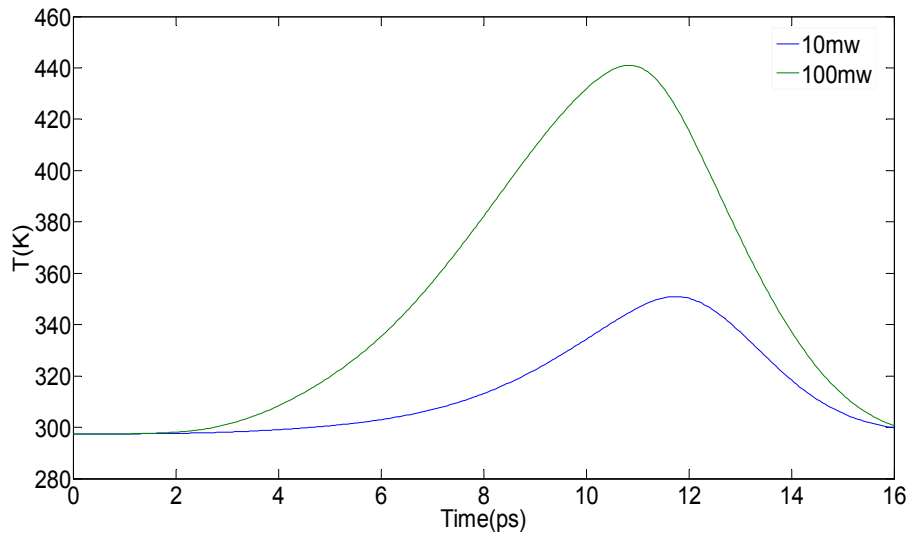


Fig.6 Average carrier temperature of the amplifier cavity in picosecond pulse amplification process with the input peaks 10mw and 100mw

Figure 6 shows the average carrier temperature of the amplifier cavity during the pulse propagation. The initial lattice temperature is 300K and the time on the x-axis means the optical signal begins to enter the amplifier. The results indicate that the carrier temperature hardly changes when $t < 4ps$ this is because the propagation and amplification of the input pulse needs time. When $t > 4ps$, due to the large optical field (stimulated emission) and the free carrier absorption in the amplification cavity, the rates of energy and carrier density changes are high. The highest temperatures are 350.9K (GP-1) and 441.1K (GP-2). When the input peak value is 100mw, the carrier temperature arrives at the peak point earlier. This is because a smaller amplification has saturated the amplifier when the input power is higher.

4 Conclusion

In this paper, we have presented a new method to analyse carrier heating effects in QW-SOAs considering the discontinuous distribution of energy band structure and the coupling among heavy hole bands and light hole bands as well as spin-orbit split-off bands. Based on the analysis of energy band structure, the conduction and valence band structures for compressively strained quantum wells are obtained. The modal gain spectra and the spontaneous emission spectra were investigated at different temperatures. It has been shown that as the temperature increases, the modal gain spectrum values and the spontaneous emission spectrum values descend due to the decrease of the Fermi level in the conduction band and the increase of the Fermi level in the valence band. A small blue shift appears in the modal gain spectrum. We have also investigated the picoseconds pulse amplification in QW-SOAs by considering the carrier heating effects. The results showed that carrier heating effects have significantly distorted the amplified output pulse and hence broadened it.

Reference

- Agrawal, G.P., Olsson, N.A.: Amplification and compression of weak picosecond optical pulses by using semiconductor laser amplifiers. *Opt. Lett.*, **14**, 500 (1989)
- Chuang, S.L.: *Physics of Optoelectronic Devices*, New York (1995).
- Chang, C., Chuang, S.: Modeling of strained quantum-well lasers with spin-orbit coupling. *IEEE J. Sel. Topics Quantum Electron.*, **1**, 218 (1995)
- Chao, C.Y.P., Chuang, S.L.: Spin-orbit-coupling effects on the valence-band structure of strained semiconductor quantum wells. *Phys Rev E*, **46**, 4110 (1992)
- Chuang, S.L.: Efficient band-structure calculations of strained quantum wells. *Phys. Rev. B*, **43**, 9649 (1991)
- Connelly, M.J.: Wideband semiconductor optical amplifier steady-state numerical model. *IEEE J. Quantum Electron.*, **37**, 439 (2001)
- Dailey, J.M., Koch, T.L.: Impact of carrier heating on SOA dynamics for wavelength conversion. *Lasers and Electro-Optics Society, 19th Annual Meeting of the IEEE*, 2006.
- Dailey, J.M., Koch, T.L.: Impact of carrier heating on SOA transmission dynamics for wavelength conversion. *IEEE Photon. Technol. Lett.*, **19**, 1078 (2007)

Dailey, J., Koch, T.: Simple rules for optimizing asymmetries in SOA-based Mach-Zehnder wavelength converters. *Lightw. Technol.*, **27**, 1480 (2009).

Ghafouri-Shiraz, H., Tan, P.W., Aruga, T.: Picosecond Pulse Amplification in Tapered-Waveguide Laser-Diode Amplifiers. *IEEE. Selected Topics in Quantum Electron.*, **3**, 210 (1997)

Ghafouri-Shiraz, H., Tan, P. W.: Study of a novel laser diode amplifier structure. *Semicond. Sci. Technol.*, **11**, 1443 (1996)

Huang, X., Zhang, Z., Qin, C., Yu, Y., Zhang, X.: Optimized quantum-well semiconductor optical amplifier for RZ-DPSK signal regeneration. *IEEE J. Quantum Electron.*, **47**, 819 (2011)

Juodawlkis, P.W., Plant, J.J., Loh, W., Missaggia, L.J., Jensen, K.E., O'Donnell, F.J.: Packaged 1.5- μm Quantum-Well SOA with 0.8-w output power and 5.5-dB noise figure. *IEEE Photon. Technol. Lett.*, **21**, 1208 (2009)

Jongwoon, P., Xun, L., Ping, H.W.: Gain clamping in semiconductor optical amplifiers with second-order index-coupled DFB grating. *IEEE J. Quantum Electron.*, **41**, 366 (2005)

Kendall, A.: *An Introduction To Numerical Analysis* (2nd ed.), New York (1989)

Mørk, J., Mark, J., Seltzer, C.P.: Carrier heating in InGaAsP laser amplifiers due to two-photon absorption. *Appl. Phys. Lett.*, **64**, 2206 (1994)

Mørk, J., Mecozzi, A., Hultgren, C.: Spectral effects in short pulse pump-probe measurements. *Appl. Phys. Lett.* **68**, 449 (1996).

Mørk, J., Mecozzi, A.: Theory of the ultrafast optical response of active semiconductor waveguides, *Opt. Soc. Am. B.*, **13**, 1803 (1996)

O'Reilly, E.P., Adams, A.R.: Band-structure engineering in strained semiconductor lasers. *IEEE. Quantum Electron.*, **30**, 366 (1994).

Qasaimeh, O.: Analytical model for cross-gain modulation and crosstalk in quantum-well semiconductor optical amplifiers. *Lightw. Technol.*, **26**, 449 (2008).

Qin, C., Huang, X., Zhang, X.: Theoretical investigation on gain recovery dynamics in step quantum well semiconductor optical amplifiers. *IEEE J. Quantum Electron.*, **29**, 607 (2012)

Qin, C., Huang, X., Zhang, X.: Gain recovery acceleration by enhancing differential gain in quantum well semiconductor optical amplifiers. *IEEE. Quantum Electron.*, **47**, 1443 (2011)

Sun, X., Vogiatzis, N., Rorison, J.M.: Theoretical study on Dilute Nitride 1.3 μm Quantum Well semiconductor optical amplifiers: incorporation of N compositional fluctuations. *IEEE J. Quantum Electron.*, **49**, 811 (2013)

Sugawara, M., Okazalu, N., Fujii, T., Yamazalu, S.: Conduction-band and valence-band structures in strained InGaAs/InP quantum wells on (001) InP substrates. *Phys. Rev E*, **48**, 8102 (1993)

Tolstikhin, V.I., Willander, M.: Theory of hot carrier effects on nonlinear gain in GaAs-GaAlAs lasers and amplifiers. *IEEE. Quantum Electron.*, **26**, 1989 (1990)

Van de Walle, C.G.: Band lineups and deformation potentials in the model-solid theory. *Phys. Rev. B*, **39**, 1871 (1989).

Xu, J., Ding, Y., Peucheret, C., Xue, W., Seoane, J., Zsigri, B., Jeppesen, P., and Mørk, J.: Simple and efficient methods for the accurate evaluation of patterning effects in ultrafast photonic switches. *Opt. Exp.*, **19**, 155 (2011).

Zhou, E., Öhman, F., Cheng, C., Zhang, X., Hong, W., Mørk, J., Huang, D.: Reduction of patterning effects in SOA-based wavelength converters by combining cross-gain and cross-absorption modulation. *Opt. Exp.*, **16**, 21522 (2008)

Zory JR., P.S.: *Quantum well lasers*, San Diego (1993)